ResearchGate

See discussions, stats, and author profiles for this publication at: https://www.researchgate.net/publication/227562179

Extracting fracture parameters using local collocation of full-field displacement data

Article *in* Experimental Techniques · January 2008

DOI: 10.1111/j.1747-1567.1998.tb00583.x

CITATIONS
4

READS
9

2 authors, including:

Hareesh Tippur
Auburn University
141 PUBLICATIONS **2,348** CITATIONS

SEE PROFILE

Some of the authors of this publication are also working on these related projects:

The Use of Microwave Energy for Various Advanced Applications View project

All content following this page was uploaded by Hareesh Tippur on 07 October 2016.

The user has requested enhancement of the downloaded file. All in-text references underlined in blue are added to the original document and are linked to publications on ResearchGate, letting you access and read them immediately.

by H. Krishnamoorthy and H.V. Tippur

EXTRACTING FRACTURE PARAMETERS USING LOCAL COLLOCATION OF FULL-FIELD DISPLACEMENT DATA

Full-field analysis of optical data is routinely carried out for extracting crack tip parameters.[1-6] Typically, surface or thickness average measurements are analyzed using overdeterministic least-squares procedure with two-dimensional plane stress asymptotic field equations as basis functions. Commonly used linear and nonlinear algorithms in such analyses have been reviewed by Sanford.[2] Experimental simulations, however, invariably deal with finite size fracture specimens and hence three-dimensional deformations dominate the near tip region. Therefore, optical data in the close vicinity of the crack tip needs to be avoided to ensure an accurate determination of the fracture parameters.[4] In some instances, such as in case of a crack lying along an interface, three-dimensional effects prevail all along the interface in addition to the ones near the crack tip.[5] This would require data analysis in a region where higher order terms (or, nonsingular terms) may not be negligible compared to the K-dominant terms. At the present time, far-field effects are generally taken into account by using a certain number of higher order terms in the least-squares analysis by imposing restrictions such as (1) convergence of the coefficients of the dominant term (stress intensity factors) and, (2) correlation between the fitted function and the optical data. The optimal number of higher order terms needed is generally unknown and determined by trial and error. However, due to the asymptotic nature of the field equations, when a large number of higher order terms are used, solution procedure may lead to ill-conditioned matrices. Interfacial crack tip fields are particularly prone to this problem.[5] Moreover, as the data are considered from regions far from the crack tip, Williams's solution may be less appropriate.

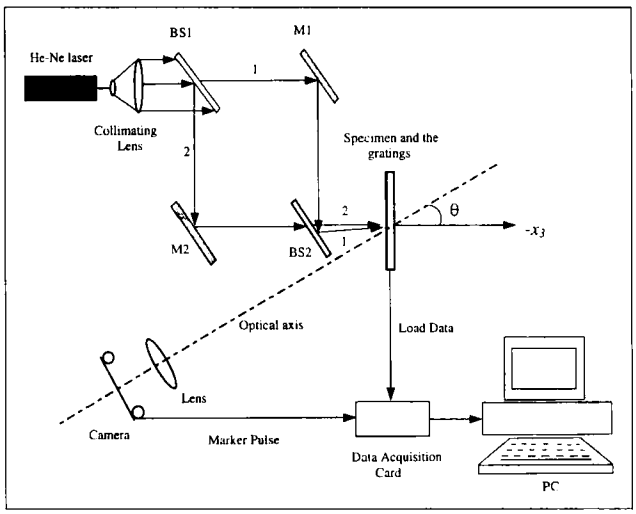

Fig. 1: Schematic of the experimental set-up for moiré interferometry

In this work, it is shown that some of the above shortcomings can be alleviated by using higher order terms that are specific to the loading configuration. Such closed form descriptions are generally available in many common fracture testing configurations. In the following, the u_2-displacement fields (displacements perpendicular to the mode-I crack plane) obtained from three-point-bending specimens are used for extracting fracture parameters in homogeneous and bimaterial beams using this modified approach.

H. Krishnamoorthy is Graduate Student, and H.V. Tippur (SEM Member) is Associate Professor, Department of Mechanical Engineering, Auburn University.

EXPERIMENTAL SETUP

The optical setup (Fig. 1) consists of an existing Mach-Zehnder interferometer[7] modified for performing moiré interferometry. The optical components include a He-Ne laser, a collimator, beam splitters—BS1 and BS2, mirrors—M1 and M2, and an imaging camera. The imaging axis of the camera makes a small angle θ (15–18 deg) with the x_3-axis in the x_2-x_3 plane. The collimated laser beam entering the interferometer is split into two paths 1 and 2 by the beam splitter BS1. The laser beams emerging from the beam splitter BS2 are made to intersect at an angle β (not shown) to create a standing wave of pitch p given by

$$p = \frac{\lambda}{2 \sin \frac{\beta}{2}} \qquad (1)$$

where λ is the wavelength of light. When a specimen with gratings of the same pitch are introduced in this space, moiré fringes are formed. Under no-load conditions, the angle β is adjusted until the pitch of the virtual gratings coincide with that of the sample gratings and a uniform light field is formed. In this paper, only fringes representing u_2-displacement components have been mapped. The displacements, the fringe orders and the pitch of the gratings are related by

$$u_2 = Np \qquad (2)$$

where N denote fringe orders (= 0, ±1, ±2, ±3, . . .).

u_2-DISPLACEMENT FRINGES AND ANALYSIS

(a) Homogeneous Fracture Tests

Aluminum beam samples of dimensions 150 mm × 12.5 mm × 5 mm with an edge notch of length 4 mm and 0.2 mm thick were made using a slitting saw. Ronchi rulings of 8 μm pitch were printed on the surface using optical lithography. The samples were subjected to monotonic, quasi-static, symmetric, three-point-bending. The u_2-displacement field and the load data were recorded. The loading configuration and a typical u_2-displacement field near the crack tip are shown in Fig. 2.

The u_2-displacements near a crack subjected to mode-I loading are described by Williams's expansion field as,[8]

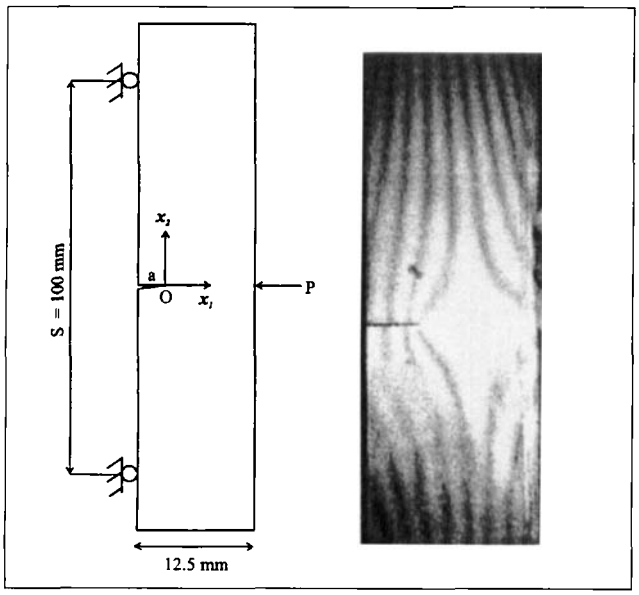

Fig. 2 Three-point-bending configuration for homogeneous specimen and u_2-displacement field

$$u_2(r, \theta) = \sum_{n=0}^{\infty} r^{n+1/2} \left\{ \frac{a_n}{\sqrt{2\pi}} u_n^I(\theta) \right\} = Np \qquad (3)$$

where (r, θ) are crack tip polar coordinates, A_n are the constant coefficients. When $n = 0, 2, 4 \ldots$,

$$u_n^I(\theta) = \frac{1}{2\mu(n+1)} \left\{ (\kappa + 1) \sin \frac{n+1}{2} \theta - (n+1) \sin \theta \cos \frac{n+1}{2} \theta \right\} \qquad (4)$$

and when $n = 1, 3, 5 \ldots$,

$$u_n^I(\theta) = \frac{1}{2\mu(n+1)} \left\{ (\kappa - 1) \sin \frac{n+1}{2} \theta - (n+1) \sin \theta \cos \frac{n-1}{2} \theta \right\} \qquad (5)$$

In eqs (4)–(5), μ is the shear modulus, and $\kappa = (3 - \upsilon)/(1 + \upsilon)$ for plane stress (υ being Poisson's ratio). Here A_0 is equal to the mode-I stress intensity factor, K_I. When all the terms $n > 0$ are neglected, eq (3) provides the so-called K-dominant description of the u_2-displacement field for the cracked body.

The fringes were digitized and fringe order and fringe location data were obtained. The x_2-coordinates of data were corrected by knowing the angle between the imaging axis and the x_3-axis. Recognizing the finite root-radius of the crack and the existence of a region of dominant three-dimensional deformations near the crack tip,[3,4] only the data in the region $r/B \geq 0.5$ (B is the sample thickness) was used in the analysis. The fracture parameters were extracted using overdeterministic least-squares analysis wherein terms from eq (3) were used as the basis functions. Denoting the right-hand sides of eq (3) by Y and F respectively, the function $\Phi = \sum_{i=1}^{M} [Y_i - F_i]^2$, is minimized with respect to the unknown coefficients A_n using single value decomposition for solving the linear system of equations. Here M represents the total number of data points used in the analysis. The analysis was first carried out under the assumption of K-dominance ($n = 0$). The corresponding match between the experimental data and the least-squares fit is shown in Fig. 3(a). The disagreement between the two is rather significant and is attributed to the higher order terms unaccounted for in the analysis. Further, the extracted value of $K_I = 13.0 \pm 0.5$ MPa$\sqrt{\text{m}}$ differs from the boundary collocation results[7] of 16.9 MPa$\sqrt{\text{m}}$ reported in the literature. It should be noted here that three-point-bend specimens generally have a much smaller region of K-dominance compared to other configurations, say, single or double edge notched sheets subjected tension. Next, the higher order terms were sequentially added until good agreement between the least-squares fit and the data was realized. In this case $n = 3$ was found adequate for representing the data. When more higher order terms were added, K_I became unstable and the match between the experimental and the least-squares fit deteriorated. The stress intensity factor obtained from the full-field analysis with $n = 3$ is $K_I = 15.9 \pm 0.5$ MPa$\sqrt{\text{m}}$, a substantial improvement compared to the K-dominant case. In Fig. 3(b), the match between the optical data and the least-squares analysis are shown and noticeable improvement can be seen.

From the full-field data in Fig. 2 it can be seen that equally spaced fringes parallel to the beam axis away from the crack tip, resemble the ones we expect for an uncracked beam subjected to three-point-bending. The influence of beam deformations near the crack tip are also evident from the fringe pattern. It suggests that well known elasticity solutions for an uncracked beam can be used as higher order terms for analyzing the data. The functional form of the higher order terms from flexural analysis[8] can be derived as follows.

$$u_2^{(beam)} = C_1(x_1 - l)x_2 + C_2(x_1 - l)x_2^2 + C_3 \qquad (7)$$

where l is the shift in the coordinates between the uncracked beam coordinates (X_1, X_2) and the crack tip coordinates (x_1, x_2). In eq (7), C_1, C_2, C_3 are constant coefficients. Using the boundary condition for this problem, i.e., $u_2 = 0$ when $x_2 = 0$, we get $C_3 = 0$. Therefore, the K-dominant term in eq (3) was used along with eq (7) as basis functions in the least-squares analysis to extract K_I:

$$u_2 = r^{1/2} \frac{K_I}{\sqrt{2\pi}} u_0^I(\theta) + C_1(x_1 - l)x_2 + C_2(x_1 - l)x_2^2 \qquad (8)$$

The results obtained from eq (8) are shown in Fig. 4. Evidently, the agreement between the optical data and the least-squares analysis is as good as in Fig. 3(b). Furthermore, K_I obtained from the analysis is 16.8 ± 0.5 MPa $\sqrt{\text{m}}$ and is in very good agreement with the published result[7] of 16.9 MPa$\sqrt{\text{m}}$. Thus, the method of using higher order terms specific to the loading configuration instead of the ones from an asymptotic field on a trial and error basis seems to be a feasible and better alternative in this case.

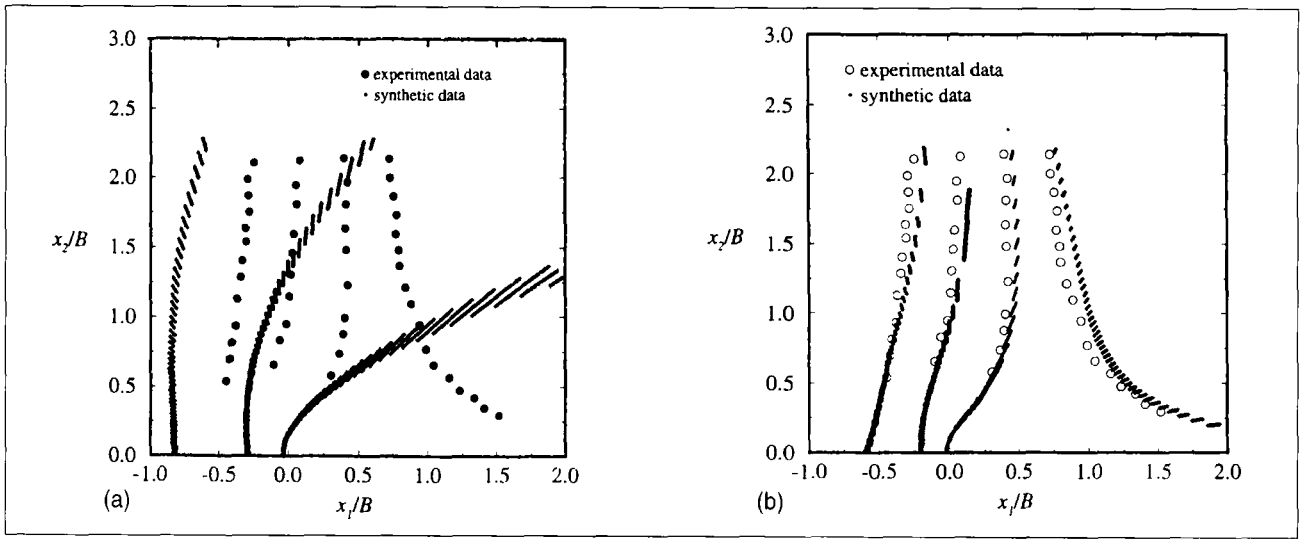

Fig. 3 Measured and synthetic u_2-displacements: (a) *K*-dominant case (n = 0) (b) with higher order terms (n = 3)

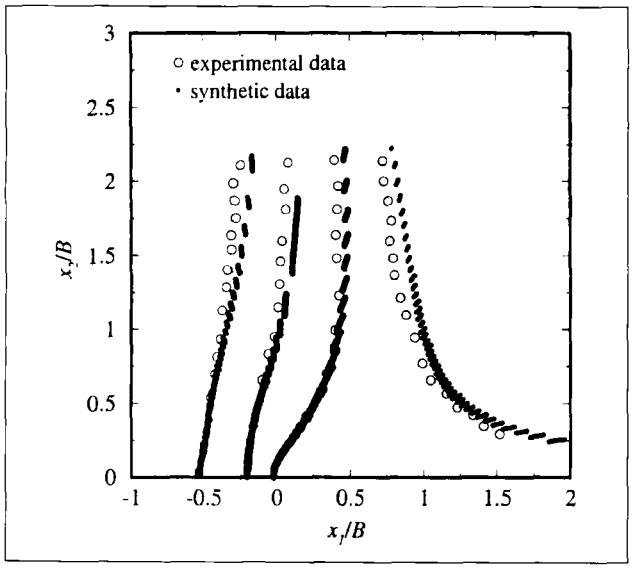

Fig. 4 Measured and synthetic u_2-displacements: *K*-dominant terms + higher order terms from an uncracked beam analysis

(b) Bimaterial Fracture Tests

Next, we consider the proposed method for interfacial crack tip parameter extraction. Bimaterial samples (150 × 25 × 5 mm) were made by bonding equal halves of aluminum and PMMA (poly-methylmethacrylate) using methylmethacrylate (MMA) monomer and a polymerizing agent.[5,6] A 50 μm thick Teflon tape was used to produce an edge crack (a/W = 0.25, W being the width of the sample). After curing, one of the faces of the bimaterial sample was polished and a thin aluminum film was deposited. Subsequently, gratings of pitch 8 μm were printed using optical lithography with grating lines parallel to the interface.

As in the previous case, the bimaterial beams were subjected to three-point-bending and u_2-displacements and the load data were acquired from no-load condition to crack initiation and growth. The loading configuration and a typical u_2-displacement field near a quasi-statistically growing interfacial crack (a = 8 mm, P = 260 N) are shown in Fig. 5. It should be noted that although the loading is nearly symmetric, the elastic mismatch along the interface introduces substantial asymmetry in the crack tip u_2-displacements. As one would expect, deformations dominate the PMMA half while the aluminum half undergoes a simple rotation.

The u_2-displacement fringes were digitized to gather fringe order (N) and fringe location (r, θ) data. The experimental data outside the region of dominant three-dimensional deformations[5] ($r/B > 0.5$, 135 deg $< \theta <$ 70 deg) in the $\theta >$ 0 (PMMA half) were then analyzed in an overdeterministic least-squares sense to extract the fracture parameters. The equations for the *K*-dominant u_2-displacements near an in-

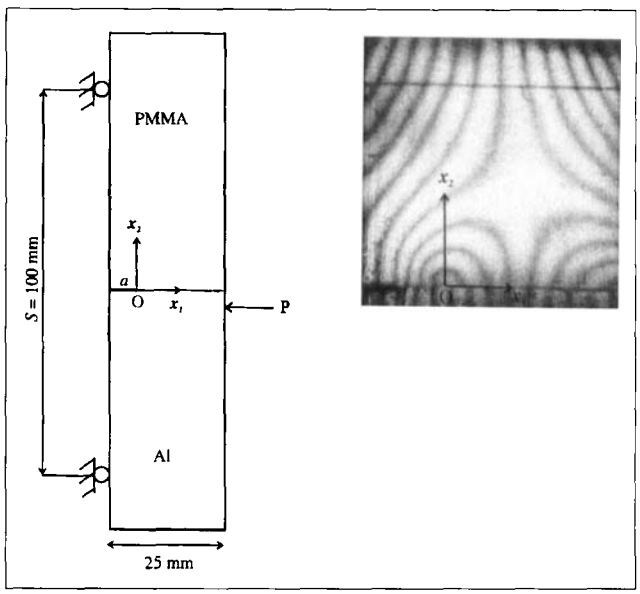

Fig. 5 Three-point-bending configuration for bimaterial specimen and u_2-displacement field

terfacial crack tip were used along with the higher order terms from beam theory as the basis functions in the least-squares analysis. Thus the u_2-displacement field can then be expressed as[10]

$$u_2(r, \theta > 0) = \frac{\sqrt{r}}{C} \times \left\{ \left[\cosh \varepsilon(\pi - \theta) + \frac{\kappa_1 - 1}{2} e^{-\varepsilon(\pi-\theta)} \right] \sin \frac{\theta}{2} - \frac{1}{2}[1 + 4\varepsilon^2] e^{-\varepsilon(\pi-\theta)} \sin\theta \cos\frac{\theta}{2} - 2\varepsilon \left[\sinh \varepsilon(\pi - \theta) - \frac{\kappa_1 - 1}{2} e^{\varepsilon(\pi-\theta)} \right] \cos\frac{\theta}{2} \right\} \mathrm{Re}(Kr^{i\varepsilon}) + \left\{ \left[\sinh \varepsilon(\pi - \theta) - \frac{\kappa_1 - 1}{2} e^{\varepsilon(\pi-\theta)} \right] \frac{\theta}{2} + \frac{1}{2}[1 + 4\varepsilon^2] e^{\varepsilon(\pi-\theta)} \sin\theta \sin\frac{\theta}{2} + 2\varepsilon \left[\cosh \varepsilon(\pi - \theta) + \frac{\kappa_1 - 1}{2} e^{-\varepsilon(\pi-\theta)} \right] \sin\frac{\theta}{2} \right\} \mathrm{Im}(Kr^{i\varepsilon}) + C_1(x_1 - l)x_2 + C_2(x_1 - l)x_2^2 + C_3 = Np \quad (9)$$

where $C = \sqrt{2\pi}\mu[1 + 4\varepsilon^2] \cosh \pi\varepsilon$. Here, $\varepsilon = \frac{1}{2\pi} \ln \frac{\mu_2\kappa_1 + \mu_1}{\mu_1\kappa_2 + \mu_2}$ (= 0.098 for PMMA-aluminum; subscripts 1, 2 represent PMMA and aluminum, respectively) is the elastic mismatch parameter and K (= $K_1 + iK_2$) is the complex stress intensity factor. The fracture parameters obtained from the full-field analysis for the case shown in Fig. 4 are $Ka^{i\varepsilon} = (1.37 - i0.2) \pm 0.1$ MPa$\sqrt{\text{m}}$. As expected, the value of $\mathrm{Re}(Ka^{i\varepsilon})$ is dominant in this example due to the tensile loading of the bimaterial beam. The experimental and the synthetic u_2-fields obtained from the above analysis are shown in Fig. 6. Good agreement between the two is evident. Furthermore, the results agree with a complementary finite element (details are avoided here for brevity) results[11] (obtained by calculating the interaction integral for the method mode-partitioning) $Ka^{i\varepsilon} = (1.46 - i0.05) \pm 0.1$ MPa$\sqrt{\text{m}}$.

CONCLUSIONS

Least-squares analysis of optically measured displacement data for extracting fracture parameters in homogeneous and bimaterial beams is discussed. The u_2-displacements measured using moiré interferometry are analyzed and fracture parameters are extracted. The feasibility of using K-dominant expressions along with the higher order terms specific to loading configuration is successfully demonstrated for the case of three-point-bending. Elasticity solution of an uncracked beam when used as higher order terms along with K-dominant terms provide accurate measurement of stress intensity factors. The method offers an alternative for using asymptotic fields for fringe analysis wherein the number of terms needed for an accurate fracture parameter extraction is generally unknown and involves a trial and error process.

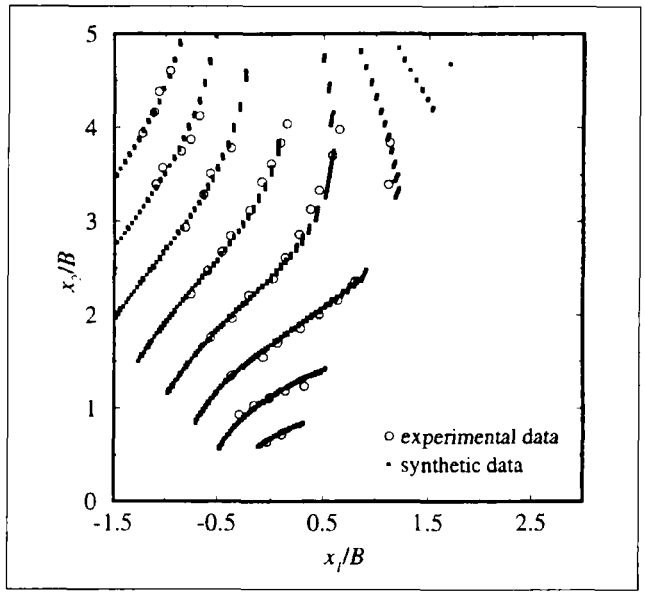

Fig. 6 Measured and synthetic u_2-displacements for an interfacial crack: K-dominant + higher order terms from uncracked beam analysis

ACKNOWLEDGMENTS

The support of the research by NSF grant CMS-9313153 is gratefully acknowledged.

References

1. Barker, D.B., Sanford, R.J. and Chona, R., 'Determining K and Related Stress-field Parameters from Displacement Fields', Experimental Mechanics, **25**(4), 399–407 (1985).

2. Sanford, R.J., 'Determining Fracture Parameters with Full-field Optical Methods', Experimental Mechanics, **29**(3), 241–247 (1989).

3. Smith, C.W., Czarnek, R., and Rezvani, M., 'Determination of Continuum Fracture Parameters for a Particulate Composite,' J. Eng. Mat. & Tech., **112**, 247–252 (1990).

4. Ramaswamy, S., Tippur, H.V. and Xu, L. 'Mixed-mode Crack-tip Deformations Studied Using a Modified Flexural Specimen and Coherent Gradient Sensing', Experimental Mechanics, **33**(3), 218–227 (1993).

5. Sinha, J.K., Tippur, H.V., and Xu, L., 'An Interferometric and Finite Element Investigation of Interfacial Crack Tip Stress Fields: Role of Mode-mixity on 3-D Stress Variations,' Int. J. Solids & Struct., **34**(6), 741–754 (1997).

6. Xu, L., and Tippur, H.V., 'Fracture Parameters for Interfacial Cracks: an Experimental Finite Element Study of Crack Tip Fields and Crack Initiation Toughness,' Int. J. Fract., **71**, 345–363 (1995).

7. Tada, H., Paris, P.C., and Irwin, G.R., 'The Stress Analysis of Cracks Handbook,' Paris Publications, Inc. (1985).

8. Williams, M.L., 'On the Stress Distribution at the Base of a Stationary Crack,' J. Appl. Mech., **24**, 109–114 (1957).

9. Timoshenko, S.P., and Goodier, J.N., *Theory of Elasticity*, McGraw-Hill Publishers (1951).

10. Williams, M.L., 'The Stresses Around a Fault or a Crack in Dissimilar Media,' Bul. Seismological Soc. of Amer., **49**(2) 199–203 (1959).

11. Butcher, R.J., 'Finite Element and Optical Investigation of Fracture Parameters in Functionally Graded Particulate Composites, M.S. Thesis, Auburn Univ. (in preparation). ■

View publication stats